Development of a DOPO-containing benzoxazine and its high-performance flame retardant copolybenzoxazines

M. Spontón, G. Lligadas, J.C. Ronda, M. Galià, V. Cádiz*

Departament de Química Analítica i Química Orgànica, Universitat Rovira i Virgili, Campus Sescelades, Marcel.lí Domingo s/n, 43007 Tarragona, Spain

ARTICLE INFO

ABSTRACT

A DOPO-containing benzoxazine, which could not be prepared by the traditional approaches, was successfully prepared from phenol, aniline and DOPO by a three-step procedure. The first step is the condensation of 2-hydroxybenzaldehyde with aniline, forming an intermediate imine. The second step is the addition of DOPO to the imine resulting a secondary amine. The third step is the ring closure condensation leading to DOPO-containing benzoxazine. All these structures were confirmed by 1D and 2D NMR spectra. The curing of mixtures of DOPO-containing benzoxazine and benzoxazine of bisphenol A has been studied. In the samples the molar ratio of benzoxazine monomers was varied to achieve different phosphorus content. The phosphorus-containing polybenzoxazines have been characterized by dynamic mechanical thermal analysis and thermogravimetric analysis. Limiting oxygen index values indicates good flame retardant properties.

1. Introduction

Polybenzoxazine as a novel phenolic type thermoset has been developed to overcome the shortcomings associated with traditional phenolic resins such as releasing condensation by-products and using strong acids as catalysts, while retaining good thermal properties and flame retardancy of phenolic resins [1]. It can be prepared from benzoxazines via thermally induced ring opening polymerisation. Benzoxazines are readily synthesized either in solution or by a melt-state reaction using a combination of a phenolic derivative, formaldehyde, and a primary amine [2]. Polybenzoxazines have not only the advantageous properties of conventional phenolic resins but also other interesting advantages such as heat resistance, superior electronic properties, low water absorption, low surface energy and excellent dimensional stability [3]. The disadvantages of the typical polybenzoxazines are the high temperature needed for complete curing and the brittleness of the cured materials that can sometimes limit their potential applications.

Polybenzoxazines with high flame retardant properties have attracted much attention owing to development demands for electronic materials. However, regardless of aromatic bisphenol or aromatic diamine-based benzoxazines, the flame retardancy of the resulting polybenzoxazines is not high enough for electronic

applications. According to the literature, the flame retardancy of polymers can be improved by incorporating bromine [4] or phosphorus units [5]. However, bromine-containing polymers may release toxic hydrogen bromide, and highly toxic compounds such as tetrabromodibenzo-p-dioxin, and tetrabromodibenzofuran during combustion. In contrast, phosphorus-based compounds give powerful flame retardancy by not only covering the outer layer of polymers with a non-flammable coating during combustion, but also releasing PO radicals, which have radical trapping ability.

The polyfunctionality required to form an infinite network structure upon benzoxazine polymerisation may be achieved through monomer synthesis utilizing either a multifunctional phenolic molecule with a monoamine or a multifunctional amine paired with a monophenol. Of these two approaches, the majority of polybenzoxazine research published today has focused on materials in which the multifunctional core is provided by the phenolic compound. Multifunctional amine based polybenzoxazines have an enormous potential in tailoring molecule structure for specific applications and benzoxazines based on difunctional [6–9], multifunctional aromatic diamines or their derivatives [10] have been discussed in the literature. Recently aromatic diamine-based benzoxazines, which could not easily be synthesized by traditional approaches, were prepared by a three-step procedure [11,12]. Moreover, in previous work we incorporated a phosphorus compound into the structure of the benzoxazine in the form of phenylphosphine oxide functional group in a diamine-based benzoxazine and synthesized bis(m-aminophenyl)methylphosphine oxide based benzoxazine (Bz-BAMPO), using this procedure [13].

* Corresponding author.
E-mail address: virginia.cadiz@urv.cat (V. Cádiz).

Since 1972, the cyclic organic phosphorus compound, 9,10-dihydro-9-oxa-10-phosphaphenanthrene-10-oxide (DOPO), and its derivatives have been used to make many synthetic resins flame retardant: for example epoxy, polyurethanes, polyesters and novolac resins. This rigid and bulky group contains an unusually highly thermally stable P–O–C bond, which can be attributed to the O=P–O group being protected by phenylene groups. In an attempt to find new phosphorus-containing benzoxazines that could find applications in flame retardant materials, the synthesis of DOPO-containing benzoxazines was reported [14–16].

Together with the structure modification by designing new benzoxazine monomers, there are other approaches for improving the performance of polybenzoxazines. One is copolymerising with epoxy resins [17–19] or copolymerising two or more than two benzoxazine monomers. In previous work, we described the synthesis of phosphorus-containing polybenzoxazines from mixtures of bis(m-aminophenyl)methylphosphine oxide based benzoxazine and benzoxazine of bisphenol A [20].

In this work a new DOPO-containing benzoxazine was synthesized from 2-hydroxybenzaldehyde, aniline and DOPO by a modified version of the above mentioned three-step procedure. Moreover polybenzoxazines with different phosphorus content were obtained by copolymerization of this DOPO-containing benzoxazine and the conventional bisphenol A-based benzoxazine. The curing behaviour of these materials was investigated by differential scanning calorimetry (DSC). Finally, the properties of the materials were evaluated by thermogravimetric analysis (TGA), dynamic mechanical analysis (DMTA) and the limiting oxygen index (LOI).

2. Experimental

2.1. Materials

The following chemicals were obtained from the sources indicated: commercial 9,10-dihydro-9-oxa-10-phosphaphenanthrene (DOPO) was donated by Aismalibar, aniline, bisphenol A, 2-hydroxybenzaldhehyde, from Aldrich. Paraformaldehyde was obtained from Probus. Bisphenol A-based benzoxazine (BA-Bz) [21] was synthesized as previously described.

All solvents were purified by standard procedures.

2.2. Synthesis of 2-[(phenylimino)methyl]phenol

In a three-neck round-bottom flask equipped with a magnetic stirrer, aniline (60 g, 0.64 mol), 2-hydroxybenzaldehyde (75 g, 0.61 mol) and ethanol were placed. The resultant mixture was stirred for 4 h at 50 °C under an argon atmosphere. The product was precipitated by adding ethanol (200 mL) and cooling the resulting solution with an ice/water bath. The solid was isolated by filtration, washed with cold ethanol, and dried at 60 °C. Thus, 96.2 g (80% yield) of yellowish powder was obtained.

^{1}H NMR (CDCl$_3$/DMSO-d_6 3/1, δ (ppm)): 13.15 (1H, s); 8.65 (1H, s); 7.42 (1H, m); 7.36 (2H, m); 7.28 (1H, t); 7.24 (3H, m); 6.85 (2H, m).

^{13}C NMR (CDCl$_3$/DMSO-d_6 3/1, δ (ppm)): 167.8 (s); 165.7 (d); 153.0 (s); 137.9 (d); 137.4 (d); 134.2 (d); 131.8 (d); 126.0 (d); 124.0 (s); 123.9 (d); 121.7 (d).

2.3. Synthesis of DOPO-containing 2-[(phenylamino)methyl]phenol (DOPO-Ph)

A solution of 2-[(phenylimino)methyl]phenol (22 g, 0.11 mol) in THF (50 mL) was added dropwise to a stirred solution of DOPO (24.1 g, 0.11 mol) in THF (50 mL) at room temperature for 1 h under argon atmosphere. The mixture was heated at 60 °C with stirring for 12 h. The resulting white precipitate was filtered and washed several times with cold THF and then dried under a vacuum to yield 41 g of DOPO-Ph as a white powder (90% yield). This product showed to be essentially a mixture of diastereomers (58% DOPO-Ph and 42% DOPO-Ph') by ^{1}H NMR and was used without further purification in the next step (see Scheme 1 for assignments)

^{1}H NMR (CDCl$_3$/DMSO-d_6 3/1, δ (ppm)): 9.0 (OH, s); 8.82 (OH', s); 7.99 (CH-12, dd); 7.90 (CH-15, dd); 7.64–7.86 (CH-22 + CH-22' + CH-15', m); 7.60 (CH-14, t); 7.51 (CH-14', t); 7.38 (CH-13, dt); 7.28–7.12 (CH-3 + CH-3' + CH-20 + CH-20' + CH-21 + CH-21' + CH-12' + CH-13', m); 7.04 (CH-19, d); 7.0–6.87 (CH-5 + CH-5' + CH-9 + CH-9', m); 6.84 (CH-19', d); 6.72–6.64 (CH-4 + CH-4' + CH-6, m); 6.55–6.47 (CH-8 + CH-8' + CH-10 + CH-10' + CH-6', m); 5.44 (CH-P', dd); 5.37 (CH-P + NH, m); 5.20 (NH', t).

^{13}C NMR (CDCl$_3$/DMSO-d_6 3/1, δ (ppm)): 154.8 (C-1, s, J_{C-P} = 22.0 Hz); 154.6 (C-1', s, J_{C-P} = 22.0 Hz); 148.8 (C-18, s, J_{C-P} = 33.0 Hz); 148.4 (C-18', s, J_{C-P} = 33.0 Hz); 145.7 (C-7, s,
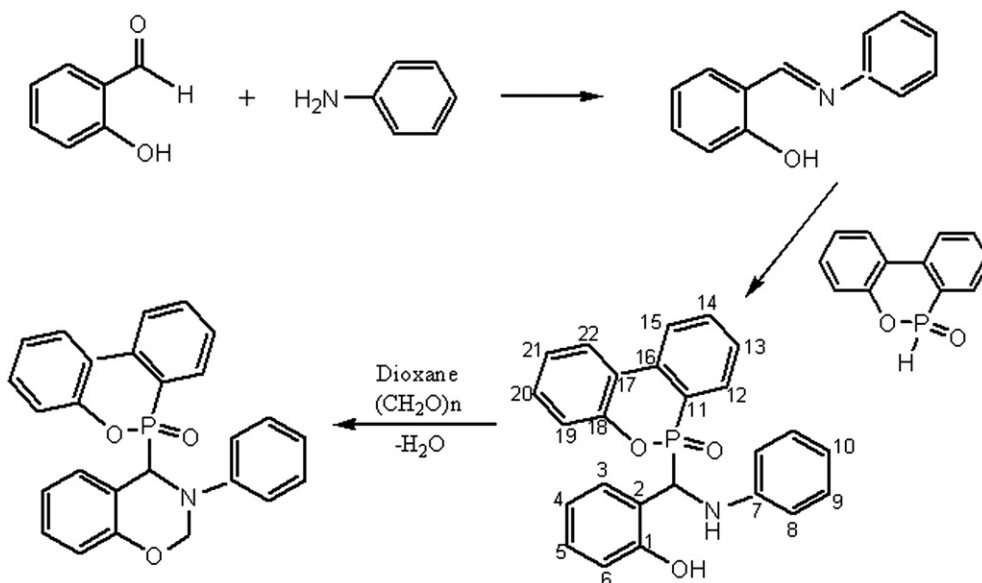
Scheme 1.

$J_{C-P} = 45.0$ Hz); 145.6 (C-7′, s, $J_{C-P} = 45.0$ Hz); 135.9 (C-17, s, $J_{C-P} = 28.0$ Hz); 135.0 (C-17′, s, $J_{C-P} = 28.0$ Hz); 132.9 (C-14, d, $J_{C-P} = 9.0$ Hz); 132.7 (C-14′, d, $J_{C-P} = 9.0$ Hz); 131.1 (C-12, d, $J_{C-P} = 38.0$ Hz); 130.5 (C-12′, d, $J_{C-P} = 38.0$ Hz); 129.8 (C-20′, d); 129.6 (C-20, d); 128.2 (C-9, d + C-5, d); 128.4 (C-3, d, $J_{C-P} = 18.0$ Hz); 127.7 (C-3′, d, $J_{C-P} = 18.0$ Hz); 127.5 (C-13, d, $J_{C-P} = 51.0$ Hz); 127.0 (C-13′, d, $J_{C-P} = 51.0$ Hz); 124.4 (C-22′, d); 124.2 (C-22, d); 123.6 (C-21′, d); 123.3 (C-21, d); 122.7 (C-15, d, $J_{C-P} = 39.0$ Hz); 122.5 (C-15′, d, $J_{C-P} = 39.0$ Hz); 122.7 (C-11, s, $J_{C-P} = 464.0$ Hz); 121.8 (C-11′, s, $J_{C-P} = 472.0$ Hz); 121.6 (C-16′, s, $J_{C-P} = 42.0$ Hz); 120.7 (C-16, s, $J_{C-P} = 42.0$ Hz); 120.1 (C-2 + C-2′, s, $J_{C-P} = 16.0$ Hz); 119.6 (C-19, d, $J_{C-P} = 25.0$ Hz); 119.5 (C-19′, d, $J_{C-P} = 25.0$ Hz); 118.8 (C-4 + C-4′, d); 117.5 (C-10, d); 117.3 (C-10′, d); 114.6 (C-6, d, $J_{C-P} = 8.0$ Hz); 114.3 (C-6′, d, $J_{C-P} = 8.0$ Hz); 113.1 (C-8, s); 113.0 (C-8′, s); 50.6 (CH-P, d, $J_{C-P} = 436.0$ Hz); 48.7 (CH-P′, d, $J_{C-P} = 413.0$ Hz).
^{31}P NMR (CDCl$_3$/H$_3$PO$_4$, δ (ppm)): 35.0; 35.8.

2.4. Synthesis of DOPO-containing 3-phenyl-3,4-dihydro-2-H-1,3-benzoxazine (DOPO-Bz)

DOPO-Ph (16.8 g, 0.04 mol) and paraformaldehyde (1.8 g, 0.06 mol) were added to a 25 mL of 1,4-dioxane, and the reaction mixture was stirred at 100 °C for 20 h. The solvent was evaporated and the residue was dissolved in dichloromethane and washed with 2 M NaOH solution. The organic layer was dried over anhydrous MgSO$_4$ and concentrated to dryness. The obtained product is a mixture of two diastereomers in a ratio 6:4. This mixture was used for the further crosslinking (see Fig. 1 for assignments).
^{1}H NMR (CDCl$_3$/DMSO-d_6 3/1, δ (ppm)): 8.06 (CH-15 + CH-15′, m); 8.02 (CH-22 + CH-22′, m); 7.83 (CH-12 + CH-12′, m); 7.70 (CH-14 + CH-14′, m); 7.49–7.37 (CH-13 + CH-13′ + CH-20 + CH-20′, m); 7.35–7.23 (CH-3 + CH-3′ + CH-21 + CH-21′ + CH-19, m); 7.12 (CH-5 + CH-19′, m); 7.08 (CH-5′, m); 7.02 (CH-9 + CH-9′, m); 6.94 (CH-4′, t); 6.84–6.77 (CH-10 + CH-10′ + CH-6 + CH-6′, m); 6.71 (CH-4, d); 6.66 (CH-8′, d); 6.59 (CH-8, d); 5.57 (O–CH–N′, d); 5.46 (O–CH–N, d); 5.14 (O–CH–N, dd); 5.11 (O–CH–N′, dd); 4.93 (CH–P′, d); 4.81 (CH–P, d).
^{13}C NMR (CDCl$_3$/DMSO-d_6 3/1, δ (ppm)): 154.3 (C-1 + C-1′, s, $J_{C-P} = 20.0$ Hz); 149.0 (C-7 + C-7′, s, $J_{C-P} = 33.0$ Hz); 148.5 (C-18 + C-18′, s, $J_{C-P} = 42.0$ Hz); 136.0 (C-17′, s, $J_{C-P} = 28.0$ Hz); 135.6

(C-17, s, $J_{C-P} = 28.0$ Hz); 133.8 (C-14 + C-14′, d); 132.0 (C-12, d, $J_{C-P} = 37.0$ Hz); 131.4 (C-12′, d, $J_{C-P} = 37.0$ Hz); 130.6 (C-20, d); 130.4 (C-20′, d); 128.7 (C-9 + C-9′, d); 128.6 (C-5, d); 128.3 (C-5′, d); 128.1 (C-13, d, $J_{C-P} = 48.0$ Hz); 128.0 (C-13′, d, $J_{C-P} = 48.0$ Hz); 127.6 (C-3 + C-3′, d); 125.0 (C-22 + C-22′, d); 124.5 (C-21 + C-21′, d); 123.5 (C-15′, d, $J_{C-P} = 38.0$ Hz); 123.4 (C-15, d, $J_{C-P} = 38.0$ Hz); 122.5 (C-10 + C-10′, d); 121.8 (C-11, s, $J_{C-P} = 420$ Hz); 121.6 (C-11′, s, $J_{C-P} = 420$ Hz); 121.4 (C-16, s, $J_{C-P} = 35.0$ Hz); 121.2 (C-16′, s, $J_{C-P} = 35.0$ Hz); 120.6 (C-4, d); 120.0 (C-4′, d); 119.8 (C-19′, d, $J_{C-P} = 26.0$ Hz); 119.6 (C-19, d, $J_{C-P} = 26.0$ Hz); 119.5 (C-8′, d); 118.8 (C-8, d); 117.1 (C-6, d); 116.9 (C-6′, d); 114.5 (C-2′, s); 114.4 (C-2, s); 77.3 (O–CH$_2$–N′, t); 76.1 (O–CH$_2$–N, t); 59.2 (CH–P, d, $J_{C-P} = 443.0$ Hz); 58.6 (CH–P′, d, $J_{C-P} = 443.0$ Hz).
^{31}P NMR (CDCl$_3$/H$_3$PO$_4$, δ (ppm)): 28.5; 31.1.

These two diastereomers present a different solubility in ethanol that allowed the separation of the predominant diastereomer (insoluble in ethanol) with high purity. This diastereomer was used as model compound for the complete and unequivocal assignments in NMR analysis.
^{1}H NMR (CDCl$_3$/DMSO-d_6 3/1, δ (ppm)): 8.04 (CH-15, dd); 7.99 (CH-22, dd); 7.81 (CH-12, dd); 7.70 (CH-14, t); 7.41 (CH-13, dd); 7.37 (CH-20, t), 7.37–7.15 (CH-3 + CH-19 + CH-21, m); 7.13 (CH-5, t); 7.01 (CH-9, t); 6.92 (CH-4, t); 6.83–6.77 (CH-10 + CH-6, m); 6.58 (CH-8, d); 5.41 (O–CH–N, d); 5.09 (O–CH–N, dd); 4.79 (CH–P, d).
^{13}C NMR (CDCl$_3$/DMSO-d_6 3/1, δ (ppm)): 154.2 (C-1, s, $J_{C-P} = 21.0$ Hz); 149.1 (C-7, s, $J_{C-P} = 33.0$ Hz); 148.5 (C-18, s, $J_{C-P} = 42.0$ Hz); 135.6 (C-17, s, $J_{C-P} = 27.0$ Hz); 133.7 (C-14, d); 132.0 (C-12, d, $J_{C-P} = 35.0$ Hz); 130.6 (C-20, d); 128.6 (C-9, d); 128.5 (C-5, d); 128.1 (C-13, d, $J_{C-P} = 48.0$ Hz); 127.5 (C-3, d, $J_{C-P} = 18.0$ Hz); 124.9 (C-22, d); 124.4 (C-21, d); 123.4 (C-15, d, $J_{C-P} = 39.0$ Hz); 122.5 (C-10, d); 121.6 (C-11, s, $J_{C-P} = 415$ Hz); 121.0 (C-16, s); 120.6 (C-4, d, $J_{C-P} = 9.2$ Hz); 119.4 (C-19, d, $J_{C-P} = 27.0$ Hz); 118.8 (C-8, d); 117.1 (C-6, d); 114.4 (C-2, s); 76.1 (O–CH$_2$–N, t); 59.5 (CH–P, d, $J_{C-P} = 443.0$ Hz).
^{31}P NMR (CDCl$_3$/H$_3$PO$_4$, δ (ppm)): 28.5.

2.5. Crosslinking reaction

Samples (Table 1) were prepared by the dissolution of DOPO-Bz and BA-Bz monomers in CH$_2$Cl$_2$. Then, this solution was evaporated at room temperature under vacuum. About 10 mg of a known weight of the mixture was put into the aluminium pan, and the polymerisation was monitored in a dynamic DSC experiment using a heating rate of 10 °C/min in a nitrogen atmosphere.

Moulded cured benzoxazine resins were prepared with a manual 15-ton hydraulic press (SPECAC) equipped with water cooled heated platens. Cured samples were compression moulded into 100 mm × 6 mm × 3 mm plaques at 160 °C for 1 h, 180 °C for 3 h, 200 °C for 1 h and 220 °C for 2 h under a pressure of 0.1 mPa.

2.6. Instrumentation

The FTIR spectra were recorded on a JASCO 680 FTIR spectrophotometer with a resolution of 4 cm^{-1} in the absorbance mode. An attenuated total reflection (ATR) accessory with thermal control and a diamond crystal (Golden Gate heated single-reflection diamond ATR, Specac. Teknokroma) was used to determine FTIR spectra. ^{1}H (400 MHz), ^{13}C (100.5 MHz) and ^{31}P (161,9 MHz) NMR spectra were obtained using a Varian Gemini 400 spectrometer with Fourier transform, CDCl$_3$/DMSO (3:1) as solvent and TMS or phosphoric acid as internal standards.

Calorimetric studies were carried out on a Mettler DSC821e thermal analyzer using N$_2$ as a purge gas (20 mL/min) at scanning rate of 10 °C/min. Thermal stability studies were carried out on a Mettler TGA/SDTA851e/LF/1100 with N$_2$ or air as a purge gas at scan rates of 10 °C/min. Mechanical properties were measured
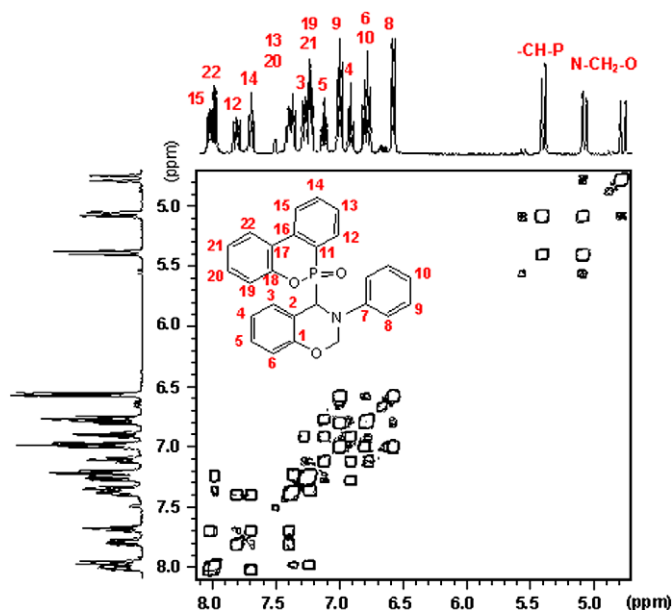

Fig. 1. ^{1}H–^{1}H COSY NMR spectrum of predominant diastereomer of DOPO-Bz.

Table 1
Characteristics of the crosslinking and Tg data of benzoxazine systems after curing.

Sample	Resin	Molar ratios resin	P%	T_{onset} (°C)[a]	T_{max} (°C)[b]	Tg (°C)[c]	Tg (°C)[d]	
							E_{max}''	Tan δ_{max}
1	DOPO-Bz	1:0	7.8	230	252	141	134	155
2	DOPO-Bz/BA-Bz	1:1	4.7	238	255	151	158	180
3	DOPO-Bz/BA-Bz	1:2	3.4	237	251	148	152	176
4	DOPO-Bz/BA-Bz	1:3	2.7	236	249	149	153	177
5	BA-Bz	0:1	–	233	245	146	154	172

[a] Initial temperature of the crosslinking exotherm.
[b] Temperature of the maximum heat release rate.
[c] Glass-transition temperature obtained by DSC.
[d] Glass-transition temperature obtained by DMTA.

using a dynamic mechanical thermal analysis (DMTA) apparatus (TA DMA 2928). Specimens (10 × 6 × 1.9 mm) were tested in a single cantilever configuration. The thermal transitions were studied in the 30–250 °C at a heating rate of 5 °C/min and at a fixed frequency of 1 Hz.

LOI values were measured on a Stanton Redcroft instrument, provided with an Oxygen Analyzer, on polymer bars that measured 100 × 6 × 3 mm and which were prepared by moulding (ASTM-D-2863).

3. Results and discussion

As is well known, benzoxazines are synthesized by the Mannich condensation of phenol, formaldehyde and amines [22]. Moreover, in an effort to minimize the generation of oligomers a three-step synthesis, through an imine intermediate which is further reduced with NaBH₄ and made to undergo cyclisation, was recently used [23,24]. This method was also successfully used in the synthesis of aromatic diamine-based benzoxazines, which could not easily be synthesized by the traditional approach [11,12,16,25]. DOPO-Bz could be synthesized using a modification of this three-step procedure presented in Scheme 1.

In the first step, 2-hydroxybenzaldehyde was reacted with aniline to give 2-[(phenylimino)methyl]phenol. According to the ^{1}H NMR data the proton aldehyde signal at 10.8 ppm disappeared but a signal at around 8.6 ppm corresponding to an imine linkage appeared, supporting the formation of the imine derivative. In the ^{13}C NMR data, the characteristic peak at around 165 ppm confirms the condensation.

It is well known that DOPO contains an active hydrogen that can easily react with electron deficient compounds. In this case DOPO

was reacted with the imine derivative at room temperature yielding the DOPO-containing phenol derivative, DOPO-Ph. In the last step paraformaldehyde in dioxane was added and the DOPO-containing benzoxazine (DOPO-Bz) was obtained with 95% of yield. As the phosphorus and the adjacent aliphatic carbon are both chiral centres, four stereoisomers were obtained. These four stereoisomers can be grouped into two pair of enantiomers resulting in two diastereomers. In the ^{31}P NMR spectrum, two peaks at 28.5 and 31.1 ppm were observed, confirming the existence of two diastereomers. These two diastereomers present a different solubility in ethanol that allowed us to separate the predominant diastereomer with high purity and complete the unequivocal assignment of the complex NMR spectra of DOPO-Bz. Figs. 1 and 2 depict the ^{1}H–^{1}H COSY and ^{1}H–^{13}C gHCQC NMR spectra of the pure predominant diastereomer. The appearance of characteristic oxazine peaks between 5.5 and 4.7 ppm, in the ^{1}H NMR spectrum, supports the formation of benzoxazine. Note that the corresponding peak of N–CH₂–O appears as two split set of signals due to the presence of magnetically non-equivalent protons.

In this work polybenzoxazines with different phosphorus content were prepared from copolymerization of DOPO-Bz and the conventional bisphenol A-based benzoxazine, BA-Bz. Table 1 summarizes the sample compositions, phosphorus content crosslinking data obtained by dynamic DSC and Tgs of the final materials measured by DSC and DMTA. DOPO-Bz and BA-Bz homopolymerizations were carried out to compare the crosslinking data and they were collected in the same table.

Fig. 3 shows the DSC plots of these systems and in Table 1 are collected the onset and maximum temperatures. As can be seen from the crosslinking exotherms, sample 1 (DOPO-Bz mixture of diastereomers), shows a broad melting process at around 170 °C
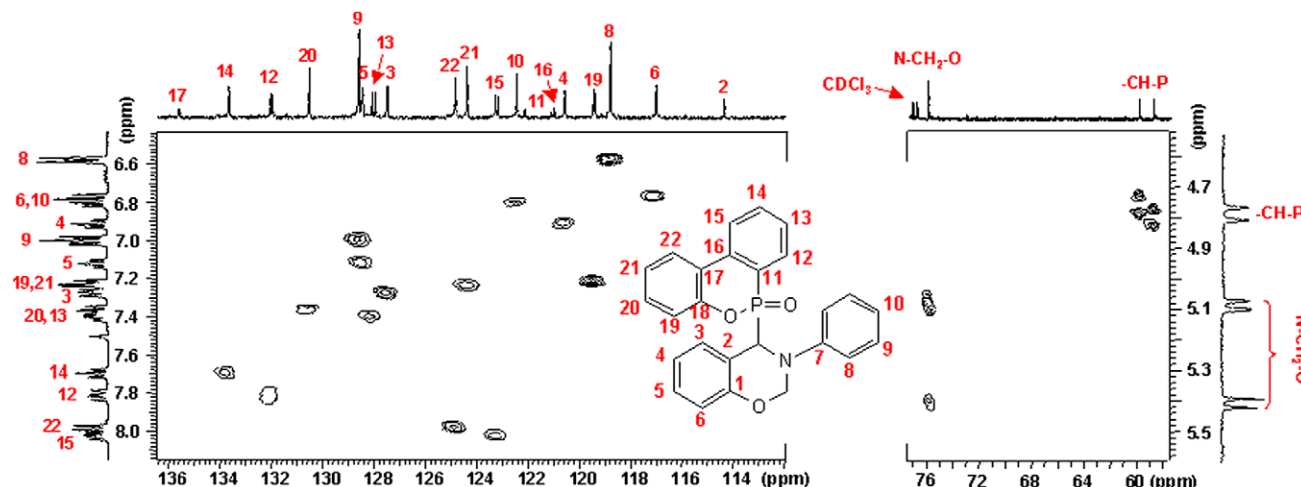

Fig. 2. ^{1}H–^{13}C gHCQC NMR spectrum of predominant diastereomer of DOPO-Bz.
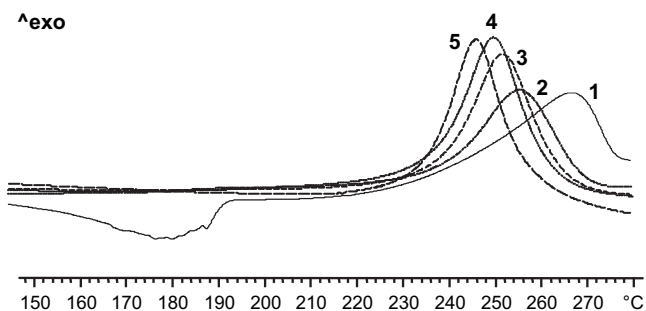
Fig. 3. DSC curves of benzoxazine systems (see Table 1).

followed by the exotherm at 252 °C due to the thermal benzoxazine ring opening. This reaction was confirmed by the disappearance of the typical signals of benzoxazine ring at between 5.6 and 4.7 ppm in its ^{1}H NMR spectrum.

BA-Bz shows a typical polymerisation exotherm for difunctional benzoxazines centred at 245 °C. No significant difference in the maximum of the polymerisation exotherms was observed in the studied compositions.

According to DSC data cured benzoxazine resins were prepared in a mould with compression (0.1 mPa) by heating samples at 160 °C for 1 h, 180 °C for 3 h, 200 °C for 1 h and 220 °C for 2 h. The Tg values could be observed in a second dynamic DSC run and are
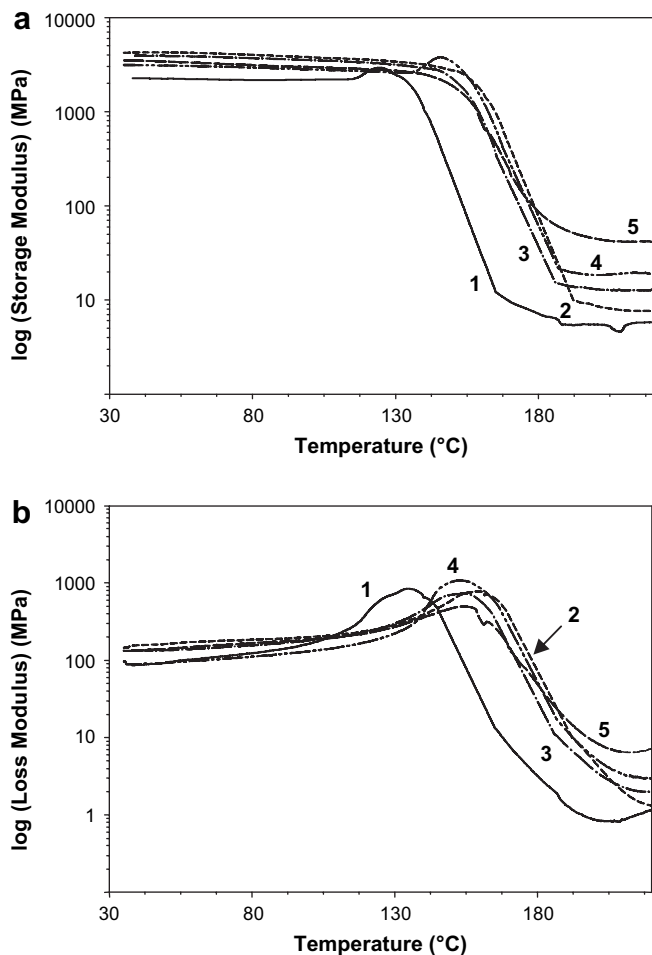
collected in Table 1. In the analysis of the Tg value there are two factors to take into account: crosslinking density, which should increase with the amount of difunctional BA-Bz, and the chemical structure of DOPO-Bz, with a strongly polar P=O group and a bulky pendant moiety, that causes restriction in the segmental mobility. Finally the combination of these two factors becomes apparent in similar Tg values about 140–150 °C for all the samples.

The dynamic mechanical and thermogravimetric properties of the polybenzoxazines were investigated. The dynamic mechanical behaviour of the cured benzoxazine resins was obtained as a function of the temperature beginning in the glassy state of each composition to the rubbery plateau of each material (Fig. 4a). The crosslinking density of a polymer can be estimated from the plateau of the elastic modulus in the rubbery state [26]. However, this theory is strictly valid only for lightly crosslinked materials, and was therefore used only to make qualitative comparisons of the level of crosslinking among the various polymers. As expected for a difunctional benzoxazine monomer, crosslinking density is higher for BA-Bz derivative than for monofunctional DOPO-Bz derivative, that shows the lowest crosslinking density. For the mixture of benzoxazine systems intermediate values are observed.

DMTA enables Tgs of the crosslinked materials to be determined. It is detected as the maximum of the loss modulus (E'), which
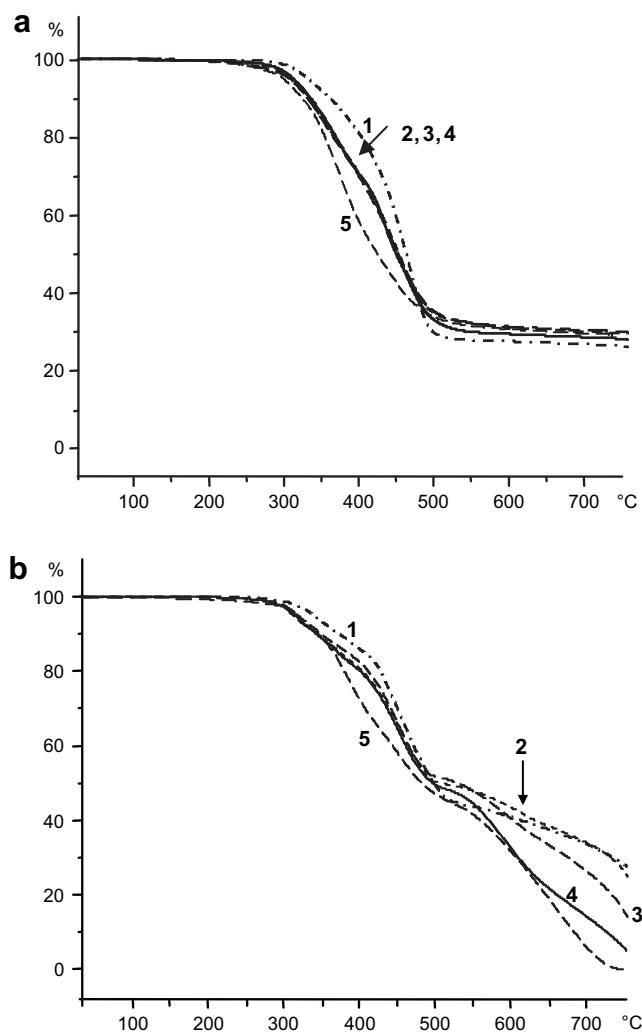

Fig. 4. Storage modulus (4a) and loss modulus (4b) as a function of the temperature of benzoxazine systems (see Table 1).

Fig. 5. TGA thermograms of polybenzoxazines under nitrogen (a) and air (b) (see Table 1).

Table 2
Thermogravimetric data in N_2 and air and LOIs of the polybenzoxazines.

Resins	P%	Nitrogen			Air				LOI, % O_2 (V/V)
		$T_{5\%}$ (°C)[a]	T_{max} (°C)[b]	Char (%)[c]	$T_{5\%}$ (°C)[a]	T_{max} (°C)[b]	T_{max} (°C)[b]	Char (%)[c]	
1	7.8	332	466	25	337	468	–	30	40.5
2	4.7	313	458	28	318	453	593	28	40.8
3	3.4	310	452	29	314	452	583	20	37.5
4	2.7	308	448	30	315	449	600	10	36.5
5	–	313	389	32	322	397	655	0	31.8

[a] Temperature of 5% weight loss.
[b] Temperature of the maximum weigh loss rate.
[c] Char yield at 750 °C.

corresponds to the initial drop from the glassy state into the transition. Moreover, the α-relaxation peak of the loss factor, tan δ, is associated with Tg and corresponds to the transition midpoint of the log of the E′ curve. The Tg values from both measurements are shown in Table 1. As expected, Tg (as tan δ peak is higher than E′ peak Fig. 4b) shows the plots of loss factor versus temperature. Table 1 shows the Tg values of both measurements. From a practical point of view, the maximum E″ is the most appropriate value since it corresponds to the highest temperature of use. As can be seen, Tg values from DMTA follow the trend above mentioned for DSC data.

To examine the effect of phosphorus content on thermal stability and the decomposition behaviour, TGA data under nitrogen and air atmospheres were determined and analysed. Fig. 5 shows the weight loss with the temperature for the different compositions under nitrogen atmosphere (Fig. 5a) and air atmosphere (Fig. 5b). Table 2 summarizes the thermogravimetric data. In nitrogen, a maximum weight loss rate appears in all cases. This behaviour indicates that there is a single decomposition mechanism which is similar for these resins. The decomposition temperature as the maximum weight loss rate of the phosphorus-free resin (389 °C) is slightly lower than those of the phosphorus-containing resins (about 450 °C). In air, a second stage of weight loss for the resins 2–5 is observed at temperatures above 500 °C indicating a more complex process than under nitrogen atmosphere. Under air, a polymeric material at these temperatures loss weight because the char formed oxidized. The weight loss rate of this second step corresponding to the thermo-oxidative degradation decreases as the phosphorus content increases and finally is not observed in resin 1 where phosphorus content is 7.8. This behaviour is in accordance with the mechanism of improved fire performance via phosphorus modification. In this retarded-degradation phenomenon, the phosphorus groups form an insulating protective layer, which prevents the combustible gases from transferring to the surface of the materials, increases the thermal stability at higher temperatures and improves the fire resistance. Under air, the char yield is low and increases significantly with the phosphorous content.

We tested the flame retardancy of the phosphorus-containing polybenzoxazines by measuring LOI values, shown in Table 2. The LOI values increased from 31.8 to around 40 when the phosphorus content increased from 0 to 7.8. As can be seen the presence of phosphorus increases the LOI values even when the phosphorus content is low, and slight differences can be observed for the higher phosphorus content resins.

4. Conclusions

DOPO-Bz was obtained as a mixture of two diastereomers showing different solubility in ethanol. This feature was used to isolate the predominant diastereomer and its NMR characterization allowed the unequivocally assignment of DOPO-Bz peaks in NMR spectra. DOPO-Bz shows a DSC pattern typical of benzoxazines with similar polymerisation exotherm than BA-Bz. Phosphorus-containing polybenzoxazines can be prepared from mixtures of this new DOPO-Bz and BA-Bz. Thermosets with enhanced LOI values were obtained confirming their good flame retardant properties.

References

[1] Ghosh NN, Kiskan B, Yagci Y. Polybenzoxazines – new high performance thermosetting resins: synthesis and properties. Prog Polym Sci 2007;32:1344–91.
[2] Ning X, Ishida H. Phenolic materials via ring-opening polymerization of benzoxazines: effect of molecular structure on mechanical and dynamic mechanical properties. J Polym Sci Part A Polym Chem 1994;32:1121–9.
[3] Low HY, Ishida H. A study on the volumetric expansion of benzoxazine-based phenolic resin. Macromolecules 1997;30:1099–106.
[4] Wang SC, Berman RJ, Walker LL, Mendoza A. Meta-bromobiphenol epoxy resins: applications in electronic packaging and printed circuit board. J Appl Polym Sci 1991;43:1315–21.
[5] Lu S-Y, Hamerton I. Recent developments in the chemistry of halogen-free flame retardant polymers. Prog Polym Sci 2002;27:1661–712.
[6] Shen SB, Ishida H. Synthesis and characterization of polyfunctional napthoxazines and related polymers. J Appl Polym Sci 1996;61:1595–605.
[7] Takeichi T, Kano T, Agag T. Synthesis and thermal cure of high molecular weight polybenzoxazine precursors and the properties of the thermosets. Polymer 2005;46:12172–80.
[8] Men W, Lu Z. Synthesis and characterization of 4,4-diaminodiphenyl methane-based benzoxazines and their polymers. J Appl Polym Sci 2007;106:2769–74.
[9] Men W, Lu Z. Synthesis of a novel benzoxazine precursor containing phenol hydroxyl group and its polymer. J Appl Polym Sci 2008;109:2218–23.
[10] Subrayan RP, Jones FN. Condensation of substituted phenols with hexakis (methoxymethyl)melamine: synthesis, characterization, and properties of substituted 2,4,6-tris(3,4-dihydro-1,3-(2 H)-benzoxazin-3yl)-s-triazine derivatives. Chem Mater 1998;10:3506–12.
[11] Lin CH, Chang SL, Hsieh CW, Lee HH. Aromatic diamine-based benzoxazines and their high performance thermoset. Polymer 2008;49:1220–9.
[12] Chang SL, Lin CH, Lin HT, Huang HJ, Hwang KY, Tu AP. Development of an aromatic triamine-based flame-retardant benzoxazine and its high-performance copolybenzoxazines. Eur Polym J 2009;45:680–9.
[13] Sponton M, Larrechi MS, Ronda JC, Galià M, Cádiz V. Synthesis of bis(m-aminophenyl)methylphosphine oxide based benzoxazine and study of thermal cross linking. J Polym Sci Part A Polym Chem 2008;46:7162–72.
[14] Weidmann U, Magendie F. WO/2002/057279
[15] Lin CH, Cai SX, Leu TS, Hwang TY, Lee HH. Synthesis and properties of flame-retardant benzoxazines by three approaches. J Polym Sci Part A Polym Chem 2006;44:3454–68.
[16] Lin CH, Lin HT, Chang SL, Hwang HJ, Hu YM, Taso YR, et al. Benzoxazines with tolyl, p-hydroxyphenyl or p-carboxyphenyl linkage and the structure–property relationship of resulting thermosets. Polymer 2009;50:2264–72.
[17] Jain R, Narula AK, Choudary V. Studies on curing and thermal behavior of diglycidylether of bisphenol-A and benzoxazine mixtures. J Appl Polym Sci 2007;106:3327–34.
[18] Espinosa MA, Cádiz V, Galià M. Development of novel flame-retardant thermosets based on benzoxazine-phenolic resins and a glycidyl phosphinate. J Polym Sci Part A Polym Chem 2004;42:279–89.

[19] Sponton M, Ronda JC, Galià M, Cádiz V. Development of flame retardant phosphorus- and silicon-containing polybenzoxazines. Polym Degrad Stab 2009;94:145–50.

[20] Sponton M, Ronda JC, Galià M, Cádiz V. Studies on thermal and flame retardant behaviour of mixtures of bis(m-aminophenyl)methylphosphine oxide based benzoxazine and glycidylether or benzoxazine of bisphenol A. Polym Degrad Stab 2008;93:2158–65.

[21] Ishida H, Rodríguez Y. Polymer curing kinetics of the new benzoxazine-based phenolic resin by differential scanning calorimetry. Polymer 1995;36:3151–8.

[22] Ishida H, Low HI. A study on the volumetric expansion of benzoxazine-based phenolic resin. Macromolecules 1997;30:1099–106.

[23] Andreu R, Ronda JC. Synthesis of 3,4-dihydro-2H-1,3-benzoxazines by condensation of 2-hydroxyaldehyde and primary amines: application to the synthesis of hydroxy-substituted and deuterium labelled compounds. Synt Commun 2008;38:2316–29.

[24] Andreu R, Reina JA, Ronda JC. Studies on the thermal polymerization of substituted benzoxazine monomers: electronic effects. J Polym Sci Part A Polym Chem 2008;46:3353–66.

[25] Lin CH, Chang SL, Lee HH, Chang HC, Hwang KY, Tu AP, et al. Fluorinated benzoxazines and the structure–property relationship of resulting poly-benzoxazines. J Polym Sci Part A Polym Chem 2008;46:4970–83.

[26] Tobolsky AV, Carlson DW, Indictor NJ. Rubber elasticity and chain configuration. J Polym Sci 1961;54:175–92.